Journal of Nanoparticle Research (2007) 9:117–125
DOI 10.1007/s11051-006-9176-4

Special issue: Nanoparticles and Occupational Health

Experimental study of nanoparticles penetration through commercial filter media

Seong Chan Kim, Matthew S. Harrington and David Y. H. Pui*
*Particle Technology Laboratory, Department of Mechanical Engineering, University of Minnesota, 111 Church St. S.E., Minneapolis, MN, 55455, USA; *Author for correspondence (Tel.: +64-3-364-2507; E-mail: dyhpui@tc.umn.edu)*

Received 29 August 2006; accepted in revised form 1 September 2006

Key words: nanoparticles, penetration, filtration, thermal rebound, diffusion, occupational health

Abstract

In this study, nanoparticle penetration was measured with a wide range of filter media using silver nanoparticles from 3 nm to 20 nm at three different face velocities in order to define nanoparticle filtration characteristics of commercial fibrous filter media. The silver particles were generated by heating a pure silver powder source via an electric furnace with a temperature of 870°C, which was found to be the optimal temperature for generating an adequate amount of silver nanoparticles for the size range specified above. After size classification using a nano-DMA, the particle counts were measured by an Ultrafine Condensation Particle Counter (UCPC) both upstream and downstream of the test filter to determine the nanoparticle penetration for each specific particle size. Particle sampling time continued long enough to detect more than 10^5 counts at the upstream and 10 counts at the downstream sampling point so that 99.99% efficiency can be detected with the high efficiency filter. The results show a very high uniformity with small error bars for all filter media tested in this study. The particle penetration decreases continuously down to 3 nm as expected from the classical filtration theory, and together with a companion modeling paper by Wang et al. in this same issue, we found no significant evidence of nanoparticle thermal rebound down to 3 nm.

Introduction

Nanotechnology, which involves the manipulation of matter at nanometer length scales to produce new materials, structures and devices, has the potential to start the new industrial revolution. The potential for new products leading to improvements in our lives is astounding. Nanoparticles often behave much differently than bulk samples of the same materials, resulting in unique electrical, optical, chemical, and biological properties. The special properties of nanoparticles give rise to recent concerns about the potential health hazards posed to workers or users that are exposed to them (Oberdörster, 2000; Maynard, 2003). Therefore, nanoparticle research has received considerable attention in many laboratories and industrial fields, especially for studying the health effects of nanoparticles and their control.

Filtration is the simplest and most common method for air cleaning, and aerosol filtration is used in diverse applications, such as respiratory protection, air cleaning of smelter effluent, processing of nuclear and hazardous materials, and clean rooms. However, the process of filtration is complicated, and although the general principles are well known there is still a gap between theory and experiment (Hinds, 1999). In particular, recent

modeling and experiments pointed to the potential penetration of nanoparticles through the filters due to thermal rebound. Further, nanoparticle penetration has not been shown clearly due to the difficulties of system set-up and penetration measurement. Wang and Kasper (1991) suggested a numerical model for nanoparticle penetration showing that the thermal impact velocity of a particle will exceed the critical sticking velocity in the size range between 1 and 10 nm depending sensitively on elastic and surface adhesion parameters. Ichitsubo et al. (1996) conducted an experimental work of nanoparticle penetration using wire screens, and showed the nanoparticle penetration below two nm in size was higher than the theoretical results due to the thermal rebound. Following this, Alonso et al. (1997) used a tandem DMA technique, and detected no particle bounce effects in the same size range as Ichitsubo et al. As of now, the thermal rebound effect on nanoparticle filtration is not well proven, and it is very important to study the air filtration properties of nanoparticles to determine the filtration requirements of personal protective equipment or HVAC filter.

In this study, the nanoparticle penetration test system has been established and the nanoparticle penetration was tested with a wide range of filter media (four fiberglass filter media, four electret filter media and one nanofiber filter media) using silver nanoparticles from 3 nm to 20 nm at face velocities of 5.3, 10 and 15 cm/s.

Experiments

Figure 1 shows a schematic diagram of a nanoparticle filtration test system, and it consists of a nanoparticle generation system, a size classification system and a penetration measurement system. An electric furnace is used to generate silver nanoparticles from a pure silver powder source (99.999%, Johnson Mattney Electronics), and clean compressed air is used as a carrier gas with flow rate of 3.0 lpm. The silver powder source located in the center of a heating tube is vaporized and condensed into silver nanoparticles with a wide size distribution at stainless steel tube parts. The particle size distribution can be controlled by changing the furnace temperature as shown in Figure 2. The average size and the particle number concentration of silver nanoparticles generated by the furnace increases with the furnace temperature, because at a higher temperature, the evaporation rate increases, giving rise to a larger amount of condensable vapor which allows the particles to grow to larger sizes by agglomeration and condensation (Ku & Maynard, 2006).

The silver nanoparticles are given a Boltzman charge distribution by Po-210 and classified by a differential mobility analyzer (nano-DMA, Model 3085, TSI). The neutralized silver nanoparticles (by another Po-210) are then introduced to the test filter and the number counts upstream and downstream of the filter are measured by an

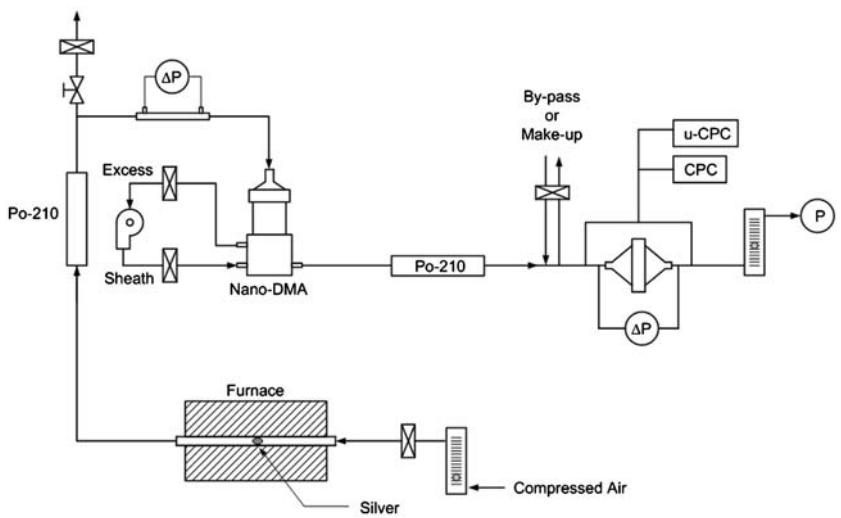

Figure 1. Schematic diagram of the nanoparticle penetration test.

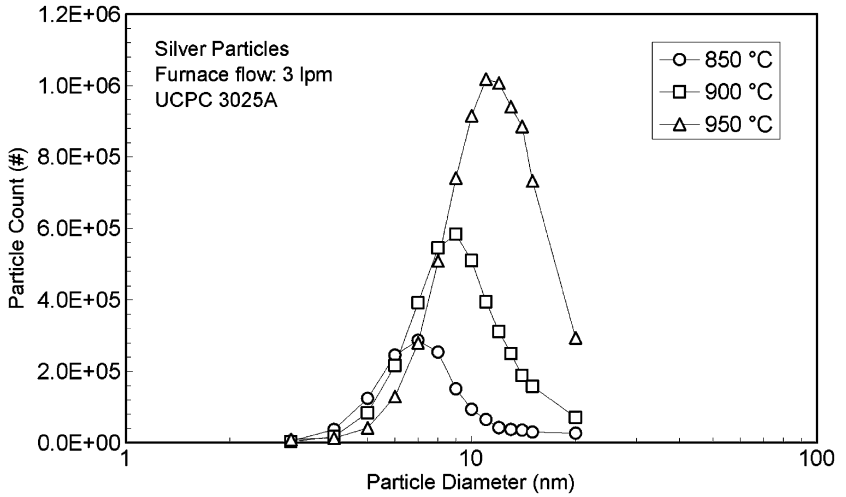

Figure 2. Silver nanoparticle size distribution as a function of temperature.

ultrafine CPC (Model 3025A, TSI) for the nanoparticle penetration calculation during a certain sampling time that is long enough to show high reliability. Each test is repeated more than five times with different test conditions to show the variability caused by the set-up and the measurement itself.

Chen et al. (1998) studied nanoparticle transportation in the nano-DMA in order to reduce nanoparticle loss and suggested a new inlet design to reduce the recirculation problem. Here, the slit width is reduced to improve the matching of the flow velocity in the classifying region and to avoid electric field penetration into the upstream side of the entrance slit. As a result, the nano-DMA has the potential for high resolution in sizing and classifying nanoparticles. Figure 3 shows the calibration results of nano-DMA measured by a Scanning Mobility Particle Sizer (SMPS, Model 3080, TSI) and CPC (Model 3022A, TSI). These size distributions were measured next to the nano-DMA for the particle size classification and the results show that nanoparticle size distribution classified by nano-DMA is monodisperse and

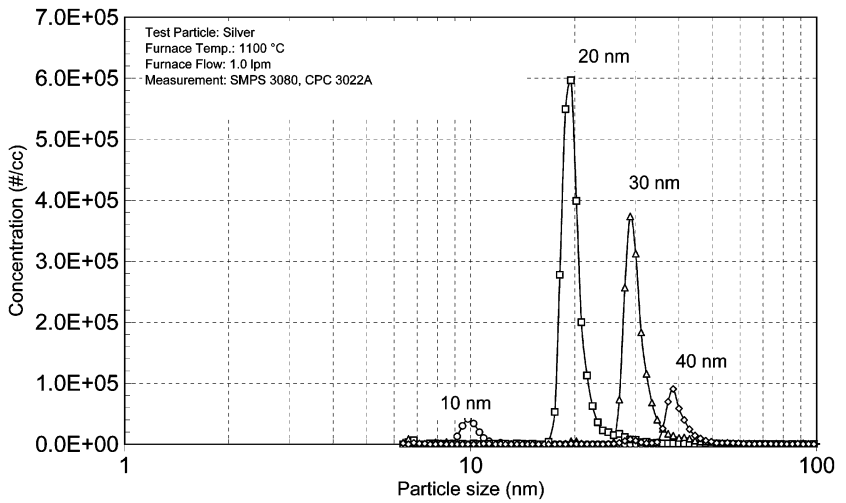

Figure 3. Nano-DMA calibration.

Table 1. Specifications of H&V fiberglass filter media

Filter Parameters		Media			
		HE1073	HE1021	HF0031	HF0012
Thickness (cm)	Ave.	0.053	0.069	0.074	0.074
	%COV	2.3	4.3	2.3	2.3
Basis Weight (g/m^2)	Ave.	63.9	80.3	82.6	69.2
	%COV	0.53	0.67	0.86	0.92
Pressure Drop at 5.3 cm/s (mmH_2O)	Ave.	8.4	4.7	3.5	1.3
	%COV	1.48	1.35	1.94	1.47
DOP % Penetration 0.3 μm at 5.3 cm/s	Ave.	12.8	39	45.8	79.9
	%COV	2.2	1.7	0.92	1.24
Fiber Density(g/m^3)	–	2.4	2.4	2.4	2.4
Solidity	–	0.050	0.049	0.047	0.039
Effective Fiber Diameter (μm)	–	1.9	2.9	3.3	4.9
Effective Pore Diameter (μm)	–	8.8	13.4	16.1	26.2

acceptable for a discrete nanoparticle penetration test.

Table 1 shows the specifications of the four different fiberglass filter media tested in this study. The filter media were made by the manufacturer, Hollingsworth and Vose of East Walpole, MA 02032, U.S.A, and were originally donated for use in the establishment of the precision and accuracy statement for the ASTM F1215-89 Standard "Standard Method for Determining the Initial Efficiency of a Flatsheet Filter Media in an Airflow Using Latex Spheres". The filter media are of very low variability, with coefficients of variation for thickness, mass per area, initial pressure drop and initial DOP penetration of less than 4, 1, 2 and 3%, respectively (Japuntich, 1991). The HE series approaches HEPA regime for small particle size and the HF series is more common to standard HVAC systems. These filter media have different combinations of supporting fibers to keep filter shape and main fibers to capture particles, and the filtration efficiency is proportional to the amount of the main fibers. Figure 4 shows the SEM images of H&V fiberglass filter media magnified 500 times. The pore size of the HE filter media is much smaller than that of the HF filter media, and the main fiber ratio of the HE filter media is much higher than that of the HF filter media.

Table 2 shows a list of commercial filter media that were tested in this study. Four different electret filter media (media A, B, C, and D) are made by the 3M Company and Lydall, Inc. and applied on commercial respirators that are widely used in the working field. Media E is a nanosized e-PTFE (expanded polytetrafluoroethylene) membrane filter medium made by W.L. Gore, and is used for ultra high efficiency filtration industrial applications. Figure 5 shows the SEM images of the commercial filter media tested in this study. The uniformity of the porosity is not as good when compared to the H&V fiberglass filter media as shown in the SEM images, but media E can be expected to show high repeatability in test results due to its uniform porosity all over the filter medium.

Each filter sample was placed in a portable filter holder with a filtration area of 17.34 cm^2, and the face velocity through the test filter medium was controlled by a regulated vacuum pump located at

Table 2. Specifications of the specialized filter media

Name	Type	Manufacturing method
Media A	Corona charged blown fiber (mid-size fiber)	Melt blowing process
Media B	Highly charged blown Fiber (mid-size fiber)	Melt blowing process
Media C	Split film fiber	Film extrusion process
Media D	Highly charged blown fiber (fine-size fiber)	Melt blowing process
Media E	e-PTFE Membrane Filter	–

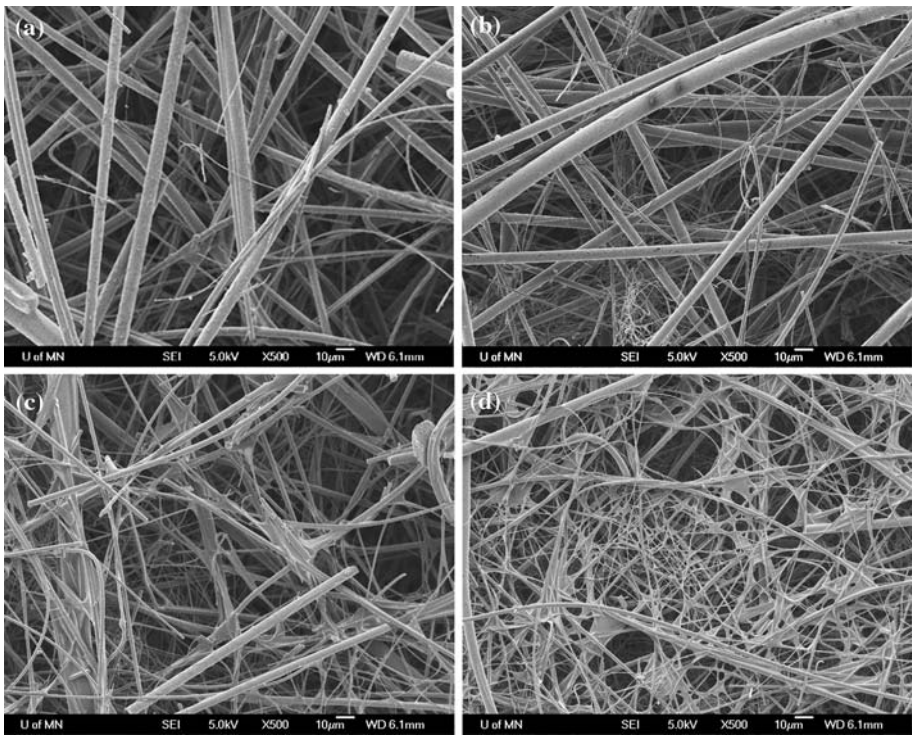

Figure 4. SEM images of the H&V filter papers (×500). (a) HF0012 (b) HF0031 (c) HE1021 (d) HE1073.

the end of the system. The tests were conducted with face velocities of 5.3, 10.0, and 15.0 cm/s. Prior to each measurement, a particle count measurement at the downstream end of the test filter with applying zero Volts to the nano-DMA was conducted in order to check the leakage of the filter holder. Because no particle can pass through the DMA without any electric field inside of the DMA, we can check a system leakage by checking the zero particle count in case of zero Volts DMA test. Furthermore, after switching the sampling point from upstream to downstream, another zero Volts DMA test was conducted to make sure that there are no residual particles inside the sampling tube.

Results and discussion

Nanoparticle penetration efficiencies were measured for four different fiberglass filter media, four different electret filter media and one nanofiber filter medium using silver nanoparticles. All experimental results are shown in terms of the percent penetration with respect to the electrical mobility diameter that is classified by the nano-DMA. Each data point is an average of at least five replicates with the maximum and minimum values as error bars. Figure 6 shows the nanoparticle penetration of the H&V fiberglass filter media at the face velocity of 5.3 cm/s, which is a standard test velocity for a respirator filter medium. The furnace setting temperature was 870°C, which can generate an adequate amount of silver nanoparticles for the size range of 3 to 20 nm. The particle sampling time was 600 s for particle sizes smaller than 5 nm and 60 s for the rest of particle size in order to get more than 10^5 counts at the upstream and 10 counts at the downstream sampling point so that 99.99% efficiency can be detected with the high efficiency filter. The results show very high uniformity with small error bars. In the case of the HF 0012, which has the lowest filtration efficiency among the H&V fiberglass filter media, data were obtainable for all particle sizes down to 3 nm, while the particle

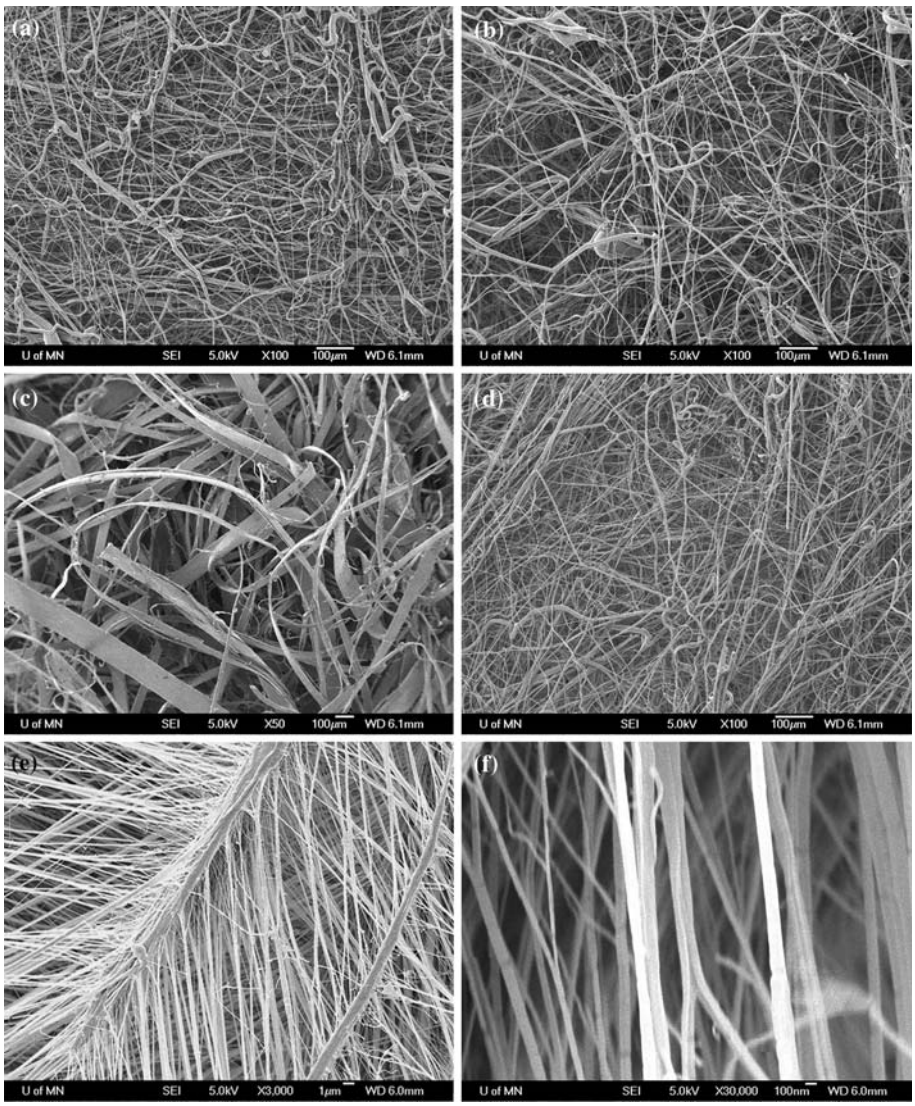

Figure 5. SEM image of the specialized filter media. (a) Media A (×100) (b) Media B (×100) (c) Media C (×50) (d) Media D (×100) (e) Media E (×3,000) (f) Media E (×30,000).

penetration less than 9 nm for the HE 1073 could not be measured due to its high filtration efficiency. In these cases, particles could not be detected at the downstream sampling point, even with an extended sampling time of 30 min. The results show that particle penetration decreases continuously down to 3 nm as expected from the classical filtration theory, and there is no significant evidence of the nanoparticle thermal rebound down to 3 nm.

Figures 7 and 8 show the nanoparticle penetration of the H&V fiberglass filter media at the face velocity of 10 and 15 cm/s, respectively. The higher face velocities show a higher penetration percentage due to a shorter residence time through the filtration region. These results show the same trend as the case of the 5.3 cm/s face velocity. Figure 9 shows the nanoparticle penetration of the commercial filter media at the face velocity of 5.3 cm/s. Nanoparticle penetration decreases

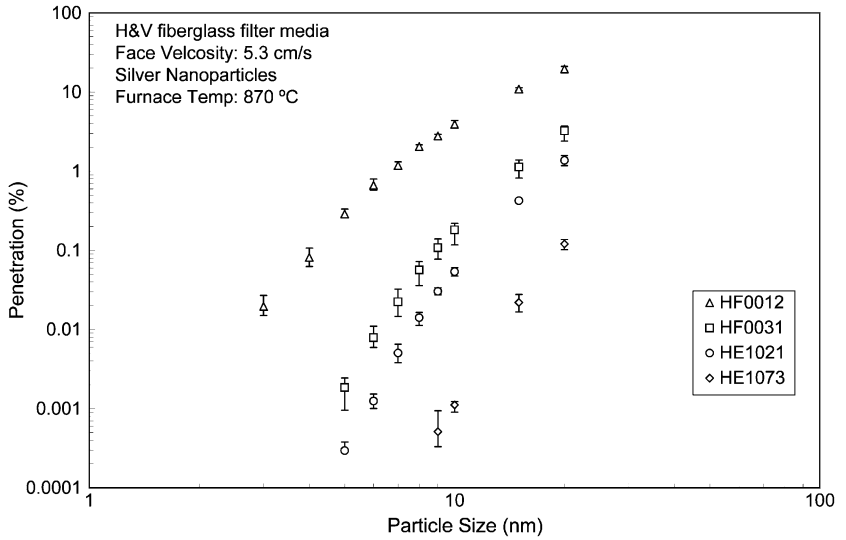

Figure 6. Nanoparticle penetration of the H&V filters at the face velocity of 5.3 cm/s.

continuously with decreasing particle size down to 3 nm with no evidence of thermal rebound. These results show larger error bars than those of the H&V fiberglass filter media due to the non-uniformity of the fiber diameter, porosity and fiber charging condition except media E as mentioned previously.

Figure 10 shows the combination of the nanoparticle penetration measured in this study with the submicron particle (from 20 to 200 nm) penetration measured by Japuntich et al. (2007) for H&V fiberglass filter media at the face velocity of 5.3 cm/s. They used a TSI 8160 automated filter tester for the particle penetration test with sodium chloride (NaCl) particles generated by an atomizer. As shown in the graph, the results agree well with each other at the particle size of 20 nm, even though different test particles were used in the

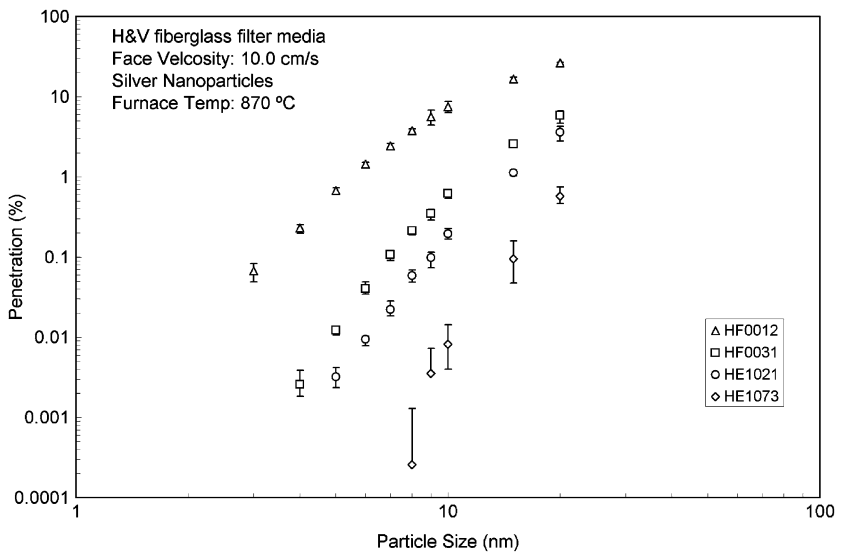

Figure 7. Nanoparticle penetration of the H&V filters at the face velocity of 10.0 cm/s.

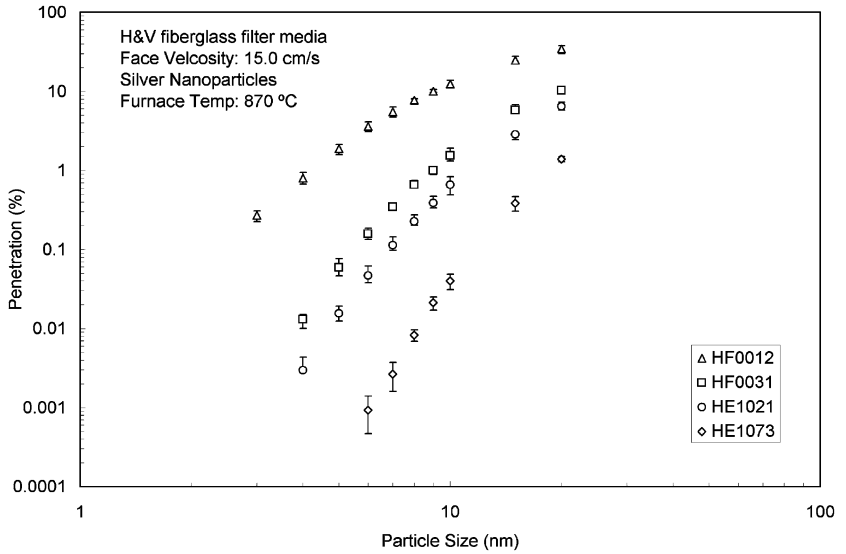

Figure 8. Nanoparticle penetration of the H&V filters at the face velocity of 15.0 cm/s.

two studies. This is because the most dominant filtration mechanism for nanoparticles is Brownian diffusion, which is not affected by the particle density.

Conclusion

In this study, the nanoparticle penetration was tested with a wide range of filter media (four glassfiber filter media, four electret filter media and one nanofiber filter medium) using silver nanoparticles from 3 nm to 20 nm at face velocities of 5.3, 10 and 15 cm/s. Nano-DMA calibration and adequate leakage tests show that the test system can produce repeatable and reliable data. The furnace setting temperature and particle sampling time were determined experimentally in order to generate enough amounts of silver nanoparticles in the size range of 3–20 nm, so that 99.99% of effi-

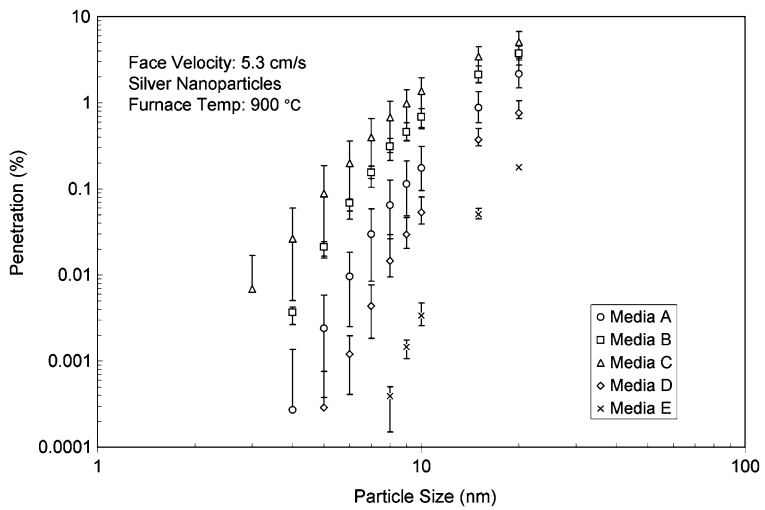

Figure 9. Nanoparticle penetration of the specialized filter media.

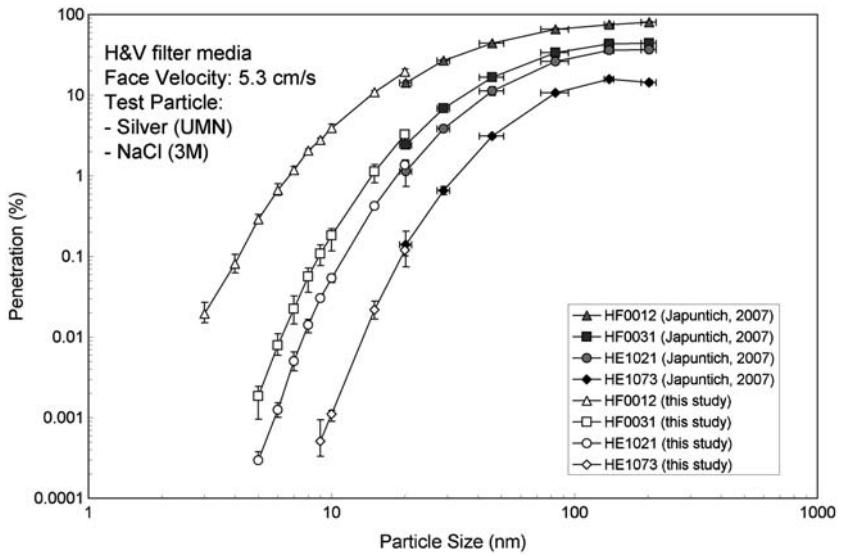

Figure 10. Comparison of test results with other study for H&V fiberglass filter media.

ciency can be measured for the high efficiency filter media. The results show a very small variability with small error bars for all filter media tested in this study, even though each test was repeated many times with a variety of test conditions (operator, test date and sample). The particle penetration decreases continuously down to 3 nm as expected from the classical filtration theory, and there is no significant evidence of nanoparticle thermal rebound down to 3 nm for nine different filter media with three different face velocities. Further, the result shows a good agreement in the overlapping size range of previous test results using submicron particles (from 20 to 200 nm).

Acknowledgement

The authors thank the support of members of the Center for Filtration Research (CFR): 3M, Donaldson, Fleetguard, Samsung Digital Appliance, Samsung Semiconductor, TSI, and W. L. Gore & Associates.

References

Alonso M., Y. Kousaka, T. Hashimoto & N. Hashimoto, 1997. Penetration of nanometer-sized aerosol particle through wire screen and laminar flow tube. Aerosol Sci. Technol. 27, 471–480.

Chen D.-R., D.Y.H. Pui, D. Hummes, H. Fissan, F.R. Quant & G.J. Sem, 1998. Design and evaluation of a nanometer aerosol differential mobility analyzer (Nano-DMA). J. Aerosol Sci. 29(5/6), 497–509.

Hinds W.C., 1999 Aerosol Technology: Properties, Behavior, and Measurement of Airborne Particles. New York: John Wiley & Sons.

Ichitsubo H., T. Hashimoto, M. Alonso & Y. Kousaka, 1996. Panetration of ultrafine particles and ion clusters through wire screen. Aerosol Sci. Technol. 24, 119–127.

Japuntich D.A., 1991 Particle Clogging of Fibrous Filters, Ph.D. Thesis. Loughborough, U.K: Loughborough University of Technology.

Japuntich, D.A., L. Franklin, D.Y.H. Pui, T. Kuehn & S.C. Kim, 2007. A comparison of two nano-sized particle air filtration tests in the diameter range of 10 to 400 nm, J. Nanoparticle Res.

Ku B.K. & A. Maynard, 2006. Generation and investigation of airborne silver nanoparticle with specific size and morphology by homogeneous nucleation, coagulation and sintering. J. Aerosol Sci. 37(4), 452–470.

Maynard A.D., 2003. Estimating aerosol surface area from number and mass concentration measurement. Ann. Occupational Hygiene 47, 123–144.

Oberdörster G., 2000. Toxicology of ultrafine particles: in vivo studies. Phil. Trans. Roy. Soc. London Ser. A 358, 2719–2740.

Wang H.-C. & G. Kasper, 1991. Filtration efficiency of nanometer-size aerosol particles. J. Aerosol Sci. 22, 31–41.